Int. J. Heat Mass Transfer. Vol. 32, No. 11, pp. 2189–2197, 1989
Printed in Great Britain

0017–9310/89 $3.00 + 0.00

Conjugate heat transfer between a laminar impinging liquid jet and a solid disk

X. S. WANG, Z. DAGAN and L. M. JIJI
Department of Mechanical Engineering, The City College of the City University of New York, Convent Ave. and 138th Street, New York, NY 10031, U.S.A.

(*Received* 6 *January* 1989 *and in final form* 3 *April* 1989)

Abstract—The conjugate heat transfer between a laminar free impinging liquid jet and a laterally insulated disk with arbitrary temperature or heat flux distribution prescribed on the non-impingement surface is investigated analytically. The local Nusselt number is found to depend upon the Prandtl number, Pr, of the fluid, the ratio of the fluid conductivity to the solid conductivity, k, the aspect ratio of the thickness to the radius of the disk, ε, and the prescribed temperature or heat flux distribution. For a thick disk, e.g. $\varepsilon = 1$, the prescribed temperature or heat flux has little effect on the local heat transfer coefficient. For a thin disk, however, the effect is considerable. Increasing the prescribed temperature or heat flux with the radial distance r from the stagnation point enhances the local heat transfer coefficient while decreasing the prescribed temperature or heat flux with r reduces it. The results also indicate that the local Nusselt number becomes higher when k is larger, other parameters being the same. For very small ε, e.g. $\varepsilon = 0.001$, the result is essentially the same as that where the boundary condition is imposed on the impingement surface (*Int. J. Heat Mass Transfer* **32**, 1361–1371 (1989)).

1. INTRODUCTION

JET IMPINGEMENT is commonly used in engineering applications because of the high heat transfer rate associated with impingement. In such applications, it is important to predict the thermal interaction between the jet and the impingement surface. To provide uniform cooling of a large surface, an array of jets is used. An understanding of the thermal characteristics of a single jet impingement is essential in optimizing the performance of multi-jet cooling units. This paper presents an analytical treatment of the conjugate problem of single jet impingement.

Laminar jet impingement heat transfer has been extensively investigated. A brief review of the previous work was given in two recent papers [1, 2]. In these two papers, analytical solutions to the problem of heat transfer between a free laminar impinging jet and a solid surface were obtained for an arbitrary surface temperature or heat flux. In the stagnation region, both the exact energy equation and the boundary layer energy equation were solved asymptotically. An integral solution was given in the transition region between the stagnation and the boundary layer regions, while in the boundary layer region, the energy equation was solved by the superposition method.

In all previous work on jet impingement heat transfer, only the energy equation for the fluid phase is solved and the boundary conditions are prescribed at the fluid–solid interface. In engineering applications of jet impingement, however, the temperature or heat flux at the impingement surface is usually unknown before the problems are solved. Consequently, the energy equations for the fluid and solid phases should be solved simultaneously.

Although most convective heat transfer problems are conjugate problems, as pointed out in ref. [3], little work has been carried out on conjugate heat transfer problems as compared to the classical convective ones in which the wall resistance is neglected. Luikov *et al.* [4] presented exact solutions to the conjugate problems of internal flow through a tube and compressible flow past a flat plate. In ref. [5], conjugate heat transfer from discrete heat sources mounted on a channel wall and exposed to fully developed laminar flow was investigated by using a finite difference method. Luikov [6] solved the conjugate heat transfer problem with a laminar incompressible flow past a flat plate of finite thickness by assuming a linear temperature distribution in the solid phase. Chung and Kassemi [7] examined the transient conjugate heat transfer for the flow over a flat plate with time-dependent temperature prescribed at the lower surface. The fluid-to-fluid conjugate heat transfer problem for a vertical pipe with forced convection inside the pipe and natural convection outside the pipe was solved numerically by Sparrow and Faghri [8]. In the analysis, the pipe wall is assumed to be very thin so that the thermal resistance of the pipe wall can be neglected.

The objective of the present paper is to investigate the conjugate heat transfer characteristics of a laminar circular jet impinging on the plane surface of a solid disk which is laterally insulated with an arbitrary temperature or heat flux distribution prescribed at the non-impingement surface. The solution is based on the analytical solutions for the fluid phase presented

NOMENCLATURE

a	constant defined in equation (5)
A_0, A_n	coefficients in the solution for the solid phase
b	constant defined in equation (20)
B_0, B_n	coefficients in the solution for the solid phase
d	jet diameter
e	parameter defined in equation (29), R_0/d
F_q	dimensionless heat flux defined in equation (26b)
F_t	dimensionless temperature defined in equation (26a)
H	thickness of the disk
k	ratio of the fluid conductivity to the solid conductivity
k_f	fluid conductivity
k_s	solid conductivity
Nu	Nusselt number, $q_i d/k_f(T_i - T_\infty)$
Pr	Prandtl number
q_i	heat flux at the interface
Q_b	prescribed heat flux at the non-impingement surface
Q_{b0}	prescribed heat flux at $r = 0$
r	radial coordinate
r_m	radial distance of the matching location
r_0	jet radius
R_0	radius of the disk
Re	Reynolds number, $U_0 d/\nu$
T_b	prescribed temperature at the non-impingement surface
T_{b0}	prescribed temperature at $r = 0$
T_f	temperature for the fluid phase
T_i	interface temperature
T_s	temperature for the solid phase
T_∞	jet temperature
T_0	stagnation point temperature
u	velocity component in the r-direction
U_0	jet exit velocity
w	velocity component in the z-direction
z	coordinate normal to the wall.

Greek symbols

α	thermal diffusivity
δ	viscous boundary layer thickness
δ_t	thermal boundary layer thickness
Δ	ratio of thermal boundary layer thickness to viscous boundary layer thickness
ε	parameter defined in equation (25a)
ζ	dimensionless variable defined in equation (25c)
θ_i	dimensionless temperature defined in equation (10)
θ_m	dimensionless temperature defined in equation (7)
θ_s	dimensionless temperature for the solid phase defined in equation (24)
λ_n	eigenvalues defined by $J_0(\lambda_n \xi_m) = 0$
ν	kinematic viscosity
ξ, ξ_m	dimensionless variables defined in equation (6)
ρ	dimensionless variable defined in equation (25b)
σ_n	eigenvalues defined by $J_1(\sigma_n) = 0$
ϕ	dimensionless function defined in equation (12).

in refs. [1, 2]. The choice of a disk for the solid phase geometry is based on the circular nature of the hydraulic jump associated with free jet impingement.

2. FORMULATION

The geometry of the present conjugate problem is shown in Fig. 1. The impinging liquid jet is laminar and the prescribed temperature T_b or heat flux Q_b is

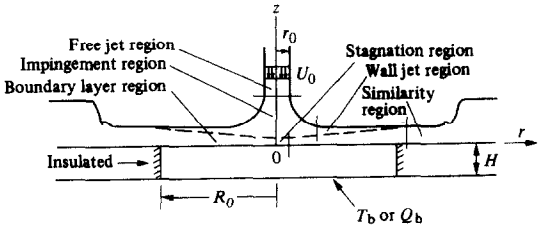

FIG. 1. Schematic diagram of a free impinging jet system.

an arbitrary function of r. The energy equation for the fluid phase is

$$u\frac{\partial T_f}{\partial r} + w\frac{\partial T_f}{\partial z} = \alpha\left(\frac{\partial^2 T_f}{\partial r^2} + \frac{1}{r}\frac{\partial T_f}{\partial r} + \frac{\partial^2 T_f}{\partial z^2}\right). \quad (1)$$

It is concluded in ref. [1] that radial conduction plays a much more important role in the stagnation region than elsewhere since the radial velocity is so small that the radial convection is negligible near the stagnation point. Consequently, the radial conduction term in equation (1) is included in the solution for the stagnation region. Outside the stagnation region, the radial velocity is well developed and hence the radial convection is much more important than the radial conduction. Consequently, the radial conduction term in equation (1) can be neglected and the temperature field is of the boundary layer type outside the stagnation region. For the solid phase, the energy equation is

$$\frac{\partial^2 T_s}{\partial r^2}+\frac{1}{r}\frac{\partial T_s}{\partial r}+\frac{\partial^2 T_s}{\partial z^2}=0. \quad (2)$$

The boundary conditions for the present conjugate problem are

$$T_f = T_\infty \quad \text{as} \quad z\to\infty \quad (3a)$$

$$\frac{\partial T_f}{\partial r}=0 \quad \text{at} \quad r=0 \quad (3b)$$

$$\frac{\partial T_s}{\partial r}=0 \quad \text{at} \quad r=0 \quad (3c)$$

$$\frac{\partial T_s}{\partial r}=0 \quad \text{at} \quad r=R_0 \quad (3d)$$

$$T_s = T_b(r) \quad \text{or} \quad -k_s\frac{\partial T_s}{\partial z}=Q_b(r) \quad \text{at} \quad z=-H \quad (3e)$$

$$T_s = T_f \quad \text{and} \quad k_s\frac{\partial T_s}{\partial z}=k_f\frac{\partial T_f}{\partial z} \quad \text{at} \quad z=0. \quad (3f)$$

3. SOLUTIONS

For conjugate problems, the energy equations for the fluid and solid phases are coupled by the matching conditions (3f) at the interface, $z=0$. Usually, to obtain an analytical solution, the general solutions to the energy equations for both phases are obtained separately. The two solutions are then matched by requiring the continuity of the temperature and heat flux at the interface.

3.1. *Solution for the fluid phase*

For the fluid phase of the present problem, the general solution to equation (1) was obtained asymptotically in ref. [1] for the stagnation region and in ref. [2] for the boundary layer region in terms of the temperature T_i at the fluid–solid interface. The solution is given in different forms for the three different regions: the stagnation region, the transition region and the boundary layer region. For the stagnation region, the heat flux at the interface is

$$q_i = -k_f\frac{T_0-T_\infty}{\sqrt{(v/a)}}\left\{\frac{\xi^2}{\xi_m^2}\theta'_m(0)+\sum_{n=1}^{\infty}[g'_n(0)+D'_n(0)]J_0(\lambda_n\xi)\right\} \quad (4)$$

where k_f and v are the conductivity and kinematic viscosity of the fluid, T_0 the stagnation point temperature, T_∞ the jet temperature, and a the velocity gradient of the potential flow given by [9]

$$a = 0.44\frac{U_0}{r_0} \quad (5)$$

where U_0 is the jet velocity and r_0 the jet radius. The dimensionless coordinate ξ is defined as

$$\xi=\frac{r}{\sqrt{(v/a)}}, \quad \xi_m=\frac{r_m}{\sqrt{(v/a)}} \quad (6)$$

where r_m is the radial distance from the stagnation point to the location at which the boundary layer thickness in the stagnation region is matched with that outside the stagnation region. The dimensionless temperature, θ_m, at the matching location is defined by

$$\theta_m=\frac{T_m-T_\infty}{T_0-T_\infty} \quad (7)$$

and g_n and D_n are determined by the following ordinary differential equations and boundary conditions:

$$g''_n+2Pr\,\phi g'_n-\lambda_n^2 g_n=0 \quad (8a)$$

$$g_n(0)=\frac{2}{\xi_m^2[J_1(\lambda_n\xi_m)]^2}\times\int_0^{\xi_m}\left[\theta_i(\xi)-\frac{\xi^2}{\xi_m^2}\theta_m(0)\right]J_0(\lambda_n\xi)\xi\,d\xi \quad (8b)$$

$$g_n(\infty)=0 \quad (8c)$$

$$D''_n+2Pr\,\phi D'_n-\lambda_n^2 D_n=L(\eta) \quad (9a)$$

$$D_n(0)=0, \quad D_n(\infty)=0 \quad (9b)$$

where

$$\theta_i=\frac{T_i-T_\infty}{T_0-T_\infty} \quad (10)$$

and

$$L(\eta)=-\frac{8\theta_m}{\xi_m^3 J_1(\lambda_n\xi_m)\lambda_n}-\frac{2}{\xi_m^2 J_1^2(\lambda_n\xi_m)\lambda_n^2}[\lambda_n\xi_m J_1(\lambda_n\xi_m)-2J_2(\lambda_n\xi_m)](\theta''_m+2Pr\,\phi\theta'_m) \quad (11)$$

while ϕ is defined by the following ordinary differential equation:

$$\phi'''+2\phi\phi''-\phi'^2+1=0 \quad (12a)$$

$$\phi(0)=\phi'(0)=0, \quad \phi'(\infty)=1. \quad (12b)$$

Finally, λ_n are the eigenvalues defined by $J_0(\lambda_n\xi_m)=0$.

For the transition region between the stagnation region and the boundary layer region, the heat flux at the interface is given by the following equation [1]:

$$q_i=2k_f\frac{T_i(r)-T_\infty}{\delta_t} \quad (13)$$

where

$$\delta_t=\Delta\delta \quad (14)$$

and δ is given by

$$\delta(r)=\sqrt{\left(\frac{420}{37}\frac{v}{U_0}r+0.81\frac{v}{U_0}\frac{r_0^3}{r^2}\right)}. \quad (15)$$

In equation (14), Δ is determined by the following ordinary differential equation:

$$\frac{\mathrm{d}}{\mathrm{d}r}\{r\delta(r)[T_i(r)-T_\infty]H(\Delta)\} = \frac{2\nu r}{U_0 Pr}\frac{T_i(r)-T_\infty}{\delta(r)\Delta} \quad (16)$$

where $H(\Delta)$ is defined as

$$H(\Delta) = \begin{cases} \frac{2}{15}\Delta^2 - \frac{3}{140}\Delta^4 + \frac{1}{180}\Delta^5 & Pr \geqslant 1 \\ \frac{3}{10}\Delta - \frac{3}{10} + \frac{2}{15\Delta} - \frac{3}{140\Delta^3} + \frac{1}{180\Delta^4} & Pr < 1. \end{cases} \quad (17)$$

For the boundary layer region, the heat flux at the interface can be written in the form [2]

$$q_i = -k_f\left[\int_{r_1}^{r}\frac{\partial}{\partial z}\theta_{st}(r,0,r^*)\frac{\mathrm{d}}{\mathrm{d}r}T_i(r^*)\,\mathrm{d}r^* - \sqrt{(3U_0/2\nu r)}\frac{T_i(r_1)-T_\infty}{\int_0^\infty \mathrm{e}^{-Pr\int_0^\eta f\,\mathrm{d}\eta}\,\mathrm{d}\eta}\right] \quad (18)$$

where r_1 can be taken as $2r_0$ according to ref. [2] and θ_{st} is the dimensionless temperature distribution corresponding to a step change in the interface temperature, $f(\eta)$ is a dimensionless function defined by

$$f''' + ff'' = 0 \quad (19a)$$

$$f(0) = f'(0) = 0, \quad f'(\infty) = 1 \quad (19b)$$

while the derivative

$$\frac{\partial}{\partial z}\theta_{st}(r,0,r^*)$$

is given by ref. [2] in the following form:

$$\frac{\partial}{\partial z}\theta_{st}(r,0,r^*) = \frac{b\sqrt{(3U_0/2\nu r)}}{(1-r^*/r)^{1/3}}[F'_0(0) + F'_1(0)(1-r^*/r) + F'_2(0)(1-r^*/r)^2 + \ldots] \quad (19c)$$

where b is a constant given by

$$b = 0.32644Pr^{1/3} \quad (20)$$

and $F'_0(0)$, $F'_1(0)$ and $F'_2(0)$ are

$$F'_0(0) = -\frac{3}{\Gamma(1/3)} \quad (21a)$$

$$F'_1(0) = -0.23329 + 0.046658Pr^{-1} \quad (21b)$$

$$F'_2(0) = -0.077764 + 0.0015553Pr^{-1} - 0.0052878Pr^{-2}. \quad (21c)$$

In all the above results, the temperature $T_i(r)$ or $\theta_i(r)$ at the interface is unknown for the present problem and should be determined by matching these results with the solution for the solid phase. In the next section, we will first obtain the general solution for the solid phase and then show how the two solutions can be matched.

3.2. *Solution for the solid phase and matching procedure*

The energy equation (2) for the solid phase can be written in dimensionless form as

$$\varepsilon^2\left(\frac{\partial^2\theta_s}{\partial\rho^2} + \frac{1}{\rho}\frac{\partial\theta_s}{\partial\rho}\right) + \frac{\partial^2\theta_s}{\partial\zeta^2} = 0 \quad (22)$$

and the boundary conditions (3) can be written in the form

$$\frac{\partial\theta_s}{\partial\rho} = 0 \quad \text{at} \quad \rho = 0 \quad (23a)$$

$$\frac{\partial\theta_s}{\partial\rho} = 0 \quad \text{at} \quad \rho = 1 \quad (23b)$$

$$\theta_s = F_t(\rho) \quad \text{or} \quad \frac{\partial\theta_s}{\partial\zeta} = -F_q(\rho) \quad \text{at} \quad \zeta = -1 \quad (23c)$$

$$T_s = T_f \quad \text{and} \quad k_s\frac{\partial T_s}{\partial z} = k_f\frac{\partial T_f}{\partial z} \quad \text{at} \quad z = 0 \quad (23d)$$

where θ_s is the dimensionless temperature for the solid phase defined by

$$\theta_s = \begin{cases} \frac{T_s - T_\infty}{T_{b0} - T_\infty} & \text{for a prescribed temperature} \\ \frac{k_s(T_s - T_\infty)}{Q_{b0}H} & \text{for a prescribed heat flux} \end{cases} \quad (24)$$

and ε, ρ and ζ are the dimensionless parameter and dimensionless coordinates defined by

$$\varepsilon = \frac{H}{R_0} \quad (25a)$$

$$\rho = \frac{r}{R_0} \quad (25b)$$

$$\zeta = \frac{z}{H} \quad (25c)$$

where R_0 and H are the radius and thickness of the disk. In equation (24), T_{b0} and Q_{b0} are the prescribed temperature and heat flux at $r = 0$, and $F_t(\rho)$ and $F_q(\rho)$ the prescribed dimensionless temperature and heat flux defined by

$$F_t(\rho) = \frac{T_b - T_\infty}{T_{b0} - T_\infty} \quad (26a)$$

$$F_q(\rho) = \frac{Q_b}{Q_{b0}} \quad (26b)$$

where T_b and Q_b are the arbitrarily prescribed temperature and heat flux. Note that the matching condition (23d) is given in dimensional form since for the fluid phase, the dimensionless temperature is defined in different forms for different regions. The solution

of equation (22) which satisfies boundary conditions (23a) and (23b) is

$$\theta_s = A_0\zeta + B_0 + \sum_{n=1}^{\infty} [A_n \cosh \varepsilon\sigma_n(\zeta+1) + B_n \sinh \varepsilon\sigma_n(\zeta+1)] J_0(\sigma_n\rho) \quad (27)$$

where σ_n are the roots of $J_1(\sigma_n) = 0$ and the coefficients A_n and B_n, $n = 0, 1, 2, \ldots$, can be determined by applying boundary condition (23c) and matching conditions (23d). Since the solution for the fluid phase is complicated, not all the coefficients can be written in explicit form. Hence an iteration procedure must be developed to determine some of the coefficients numerically. As was pointed out in refs. [8, 10], for conjugate problems the iteration procedure converges more rapidly if the thermal information is transferred through the interface by the heat transfer coefficient. The reason is that at any stage of the iteration, the heat transfer coefficient is usually closer to the correct value than the interface temperature or heat flux. In the present problem, therefore, the iteration procedure begins with guessing the Nusselt number between the jet and the disk. Then the condition at the fluid–solid interface becomes

$$\frac{\partial\theta_s}{\partial\zeta} = -\varepsilon ek\, Nu(\rho)\theta_s \quad \text{at} \quad \zeta = 0 \quad (28)$$

where $Nu(\rho)$ is the guessed Nusselt number and e and k are dimensionless parameters defined by

$$e = \frac{R_0}{d} \quad (29a)$$

$$k = \frac{k_f}{k_s}. \quad (29b)$$

The determination of the constant coefficients A_n and B_n is now described for two distinct cases. For the prescribed heat flux at the non-impingement surface, the application of boundary condition (23c) gives A_0 and B_n as follows:

$$A_0 = -2\int_0^1 F_q(\rho)\rho\, d\rho \quad (30a)$$

$$B_n = -\frac{2}{\varepsilon\sigma_n J_0^2(\sigma_n)}\int_0^1 F_q(\rho)J_0(\sigma_n\rho)\rho\, d\rho. \quad (30b)$$

Applying condition (28), one can find that A_n is determined by the following equation:

$$\sum_{n=1}^{\infty} A_n \int_0^1 S_1 J_0(\sigma_j\rho)\rho\, d\rho = \int_0^1 S_2 J_0(\sigma_j\rho)\rho\, d\rho \quad j = 1, 2, 3, \ldots \quad (31)$$

where

$$S_1 = [\varepsilon ek\, Nu(\rho)\cosh\varepsilon\sigma_n + \varepsilon\sigma_n \sinh\varepsilon\sigma_n] J_0(\sigma_n\rho) - 2\varepsilon\sigma_n\, Nu(\rho)\sinh\varepsilon\sigma_n \int_0^1 \frac{J_0(\sigma_n\rho)}{Nu(\rho)}\rho\, d\rho \quad (32)$$

and

$$S_2 = 2A_0\, Nu(\rho)\int_0^1 \frac{\sigma}{Nu(\rho)}d\rho - A_0 - \sum_{n=1}^{\infty} B_n \left\{[\varepsilon ek\, Nu(\rho)\sinh\varepsilon\sigma_n + \varepsilon\sigma_n\cosh\varepsilon\sigma_n]J_0(\sigma_n\rho) - 2\varepsilon\sigma_n\, Nu(\rho) \times \cosh\varepsilon\sigma_n \int_0^1 \frac{J_0(\sigma_n\rho)}{Nu(\rho)}\rho\, d\rho\right\}. \quad (33)$$

Finally, B_0 is given by

$$B_0 = -\frac{2A_0}{\varepsilon ek}\int_0^1 \frac{\rho}{Nu(\rho)}d\rho - \frac{2}{ek}\sum_{n=1}^{\infty}\sigma_n(A_n\sinh\varepsilon\sigma_n + B_n\cosh\varepsilon\sigma_n)\int_0^1 \frac{J_0(\sigma_n\rho)}{Nu(\rho)}\rho\, d\rho. \quad (34)$$

For the prescribed temperature at the non-impingement surface, the application of equations (23c) leads to the following results:

$$A_0 - B_0 = -2\int_0^1 F_t(\rho)\rho\, d\rho \quad (35a)$$

$$A_n = \frac{2}{J_0^2(\sigma_n)}\int_0^1 F_t(\rho)J_0(\sigma_n\rho)\rho\, d\rho. \quad (35b)$$

After applying condition (28), one obtains the following equations which determine B_n:

$$\sum_{n=1}^{\infty} B_n \int_0^1 S_3 J_0(\sigma_j\rho)\rho\, d\rho = \int_0^1 S_4 J_0(\sigma_j\rho)\rho\, d\rho \quad j = 1, 2, 3, \ldots \quad (36)$$

where

$$S_3 = \varepsilon[\sigma_n\cosh\varepsilon\sigma_n + ek\, Nu(\rho)\sinh\varepsilon\sigma_n] \times J_0(\sigma_n\rho) - 2\varepsilon\sigma_n\cosh\varepsilon\sigma_n \times \left[\frac{1 - 2Nu(\rho)\int_0^1 \frac{\rho}{Nu(\rho)}d\rho}{\varepsilon ek + 2\int_0^1 \frac{\rho}{Nu(\rho)}d\rho} + Nu(\rho)\right] \times \int_0^1 \frac{J_0(\sigma_n\rho)}{Nu(\rho)}\rho\, d\rho \quad (37)$$

and

$$S_4 = -\frac{2-4Nu(\rho)\int_0^1 \frac{\rho}{Nu(\rho)}\,d\rho}{1+\frac{2}{\varepsilon ek}\int_0^1 \frac{\rho}{Nu(\rho)}\,d\rho} \times \int_0^1 F_t(\rho)\rho\,d\rho - \sum_{n=1}^{\infty} A_n \left\{[\varepsilon ek\,Nu(\rho)\cosh\varepsilon\sigma_n + \varepsilon\sigma_n \sinh\varepsilon\sigma_n]J_0(\sigma_n\rho) - 2\varepsilon\sigma_n \times \left[Nu(\rho) + \frac{1-2Nu(\rho)\int_0^1 \frac{\rho}{Nu(\rho)}\,d\rho}{\varepsilon ek + 2\int_0^1 \frac{\rho}{Nu(\rho)}\,d\rho}\right] \times \sinh\varepsilon\sigma_n \int_0^1 \frac{J_0(\sigma_n\rho)}{Nu(\rho)}\rho\,d\rho\right\}. \quad (38)$$

Finally, A_0 is determined as

$$A_0 = -\frac{1}{1+\frac{2}{\varepsilon ek}\int_0^1 \frac{\rho}{Nu(\rho)}\,d\rho} \times \left[\frac{2}{ek}\sum_{n=1}^{\infty}\sigma_n(A_n\sinh\varepsilon\sigma_n + B_n\cosh\varepsilon\sigma_n) \times \int_0^1 \frac{J_0(\sigma_n\rho)}{Nu(\rho)}\rho\,d\rho + 2\int_0^1 F_t(\rho)\rho\,d\rho\right]. \quad (39)$$

If the infinite series in equations (31) and (36) are truncated after M terms, the two equations represent two systems of M linear algebraic equations for two sets of M unknowns, respectively. Once equations (31) and (36) are solved, the coefficients A_n and B_n can be determined for an arbitrarily prescribed temperature or heat flux at the non-impingement surface of the disk. Hence the temperature and heat flux at the fluid–solid interface can be calculated. The calculated interface temperature can then be used to compute the interface heat flux at the fluid phase by equations (4), (13) and (18). Finally, the computed heat flux values are compared with those at the solid phase in the corresponding regions. If the agreement is not satisfactory, the initial guess of the Nusselt number is changed according to the following iterative scheme:

$$Nu_{(n+1)} = Nu_{(n)} - \frac{1}{2}\frac{d}{k_f}\frac{q_{is}-q_{if}}{T_i - T_\infty} \quad (40)$$

where q_{is} and q_{if} denote the heat flux from the solid phase and fluid phase at the interface, $Nu_{(n+1)}$ and $Nu_{(n)}$ denote the $(n+1)$th guess and the nth guess, respectively. The above procedure is repeated until the desired accuracy is achieved.

In the present calculation, the Nusselt number is initially guessed at 21 radial points on the interface. The assumed values are then represented by a finite Fourier cosine series such that a continuous Nusselt number profile is prescribed. The comparison of the interface heat flux for the fluid phase with that for the solid phase is carried out at the same discrete points on the interface.

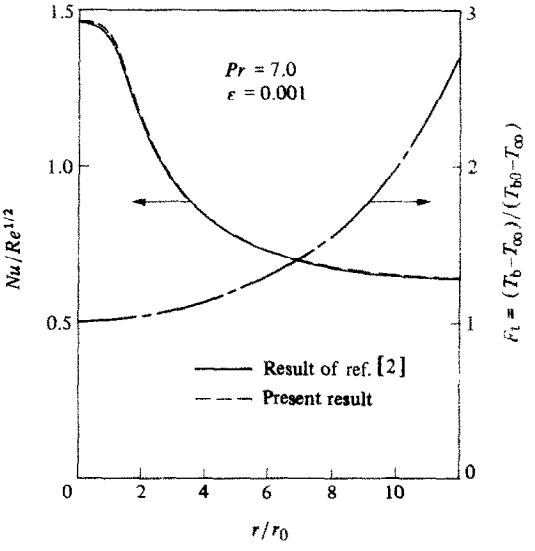

FIG. 2. Comparison with previous result.

The sensitivity of the solution to the number of points at which the Nusselt number is guessed is examined by calculating the Nusselt number for a different number of points. The calculation shows that the result is not sensitive to the number of points if the number is larger than 10. For 11 and 21 points, for instance, the difference in the Nusselt number is less than 0.5%.

4. RESULTS AND DISCUSSION

The main purpose of the present analysis is to investigate the distribution of the heat transfer coefficient between the impinging jet and the solid disk. In general, it is clear that the quantity $Nu/Re^{1/2}$ is a function of Prandtl number, Pr, the conductivity ratio, k, and the aspect ratio, ε. The prescribed temperature or heat flux profile may also influence the heat transfer coefficient distribution.

For the special case where the aspect ratio ε vanishes, the present conjugate problem becomes the convection problem of refs. [1, 2] in which the boundary conditions are prescribed at the impingement surface. For $\varepsilon = 0.001$, the present result for $Nu/Re^{1/2}$ is compared with that of ref. [2] in Fig. 2 for a prescribed increasing temperature shown in the same figure. It is clear that the present result is essentially the same as that of ref. [2] for the same prescribed temperature distribution except in a small region near the edge of the disk. This is true for any value of the conductivity ratio k. The reason for the difference near the edge is that for the conjugate problem the radial derivative of the interface temperature vanishes at the edge of the disk since it is insulated, while the derivative of

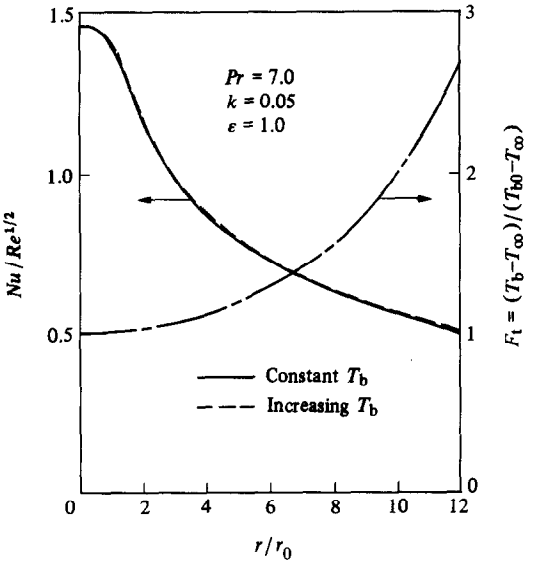

FIG. 3. Result for thick disk.

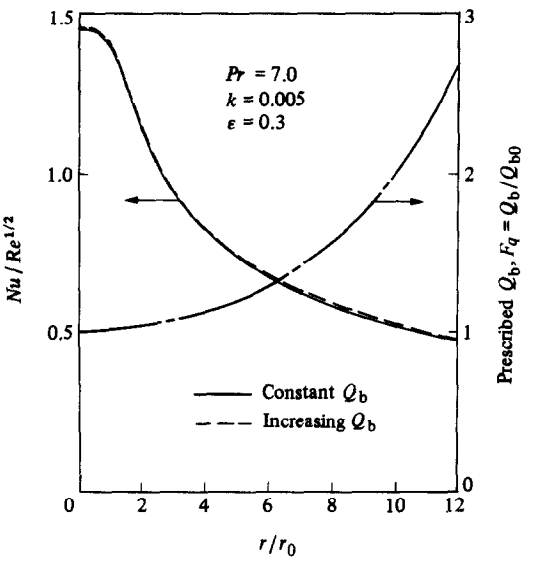

FIG. 4. Result for small k with prescribed heat flux.

the prescribed temperature is not zero at the same location. The same behavior of Nusselt number near the insulated edge was also shown in ref. [11] where the conjugate problem associated with laminar flow through a pipe was solved.

Figure 3 shows the Nusselt number profile for $\varepsilon = 1$, corresponding to the case of a thick disk. For this case, the Nusselt number is almost the same for a prescribed constant temperature and for a prescribed increasing temperature. This is due to the fact that the prescribed temperature distribution loses its influence on the interface temperature profile when the disk is sufficiently thick due to conductive effects. This is also true for the case of a prescribed heat flux distribution. As we will see later, the prescribed temperature or heat flux may affect the Nusselt number profile considerably if the disk is not very thick.

When the solid conductivity is sufficiently high, the prescribed heat flux distribution has little effect on the Nusselt number profile even for moderate disk thicknesses. This case is shown in Fig. 4 for $\varepsilon = 0.3$ and $k = 0.005$ which corresponds to a water jet impinging on a brass disk. It is seen that the Nusselt number for a prescribed constant heat flux is very close to that for a prescribed increasing heat flux. The reason is that the radial conduction in the solid phase is so severe that the dimensionless interface temperature profile is not affected by the prescribed heat flux profile when k is small. If k is reduced to 0.0001, corresponding to an air jet impinging on a copper disk, the difference in the Nusselt number is less than 0.1%. On the other hand, the prescribed temperature will affect the Nusselt number profile for the same values of ε and k. This is because the interface temperature profile always changes with the prescribed temperature profile for any value of k if the disk is not sufficiently thick.

The effect of the prescribed temperature profile on the Nusselt number distribution is shown in Fig. 5 for a moderate disk thickness. The figure indicates that the Nusselt number profile may be considerably affected by the prescribed temperature distribution. Increasing the prescribed temperature with r enhances the local Nusselt number while decreasing it reduces the local Nusselt number. The reason is that the interface temperature increases more steeply for a prescribed increasing temperature than it does for a prescribed constant temperature. Consequently, the local Nusselt number becomes higher for the prescribed increasing temperature since the steeper increase in the interface temperature results in a higher local heat transfer coefficient outside the stagnation region

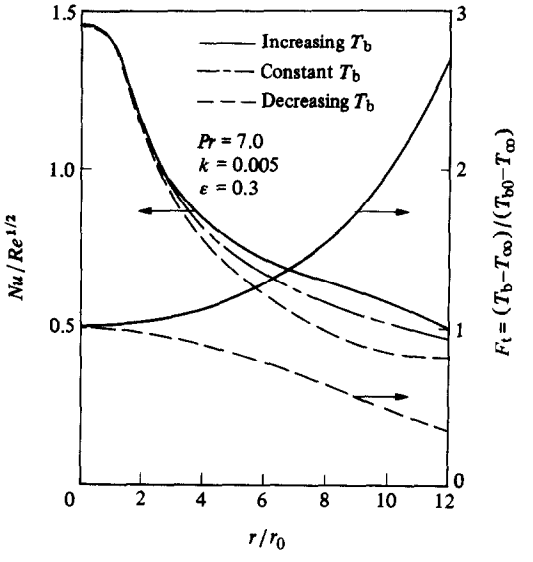

FIG. 5. Effect of prescribed temperature.

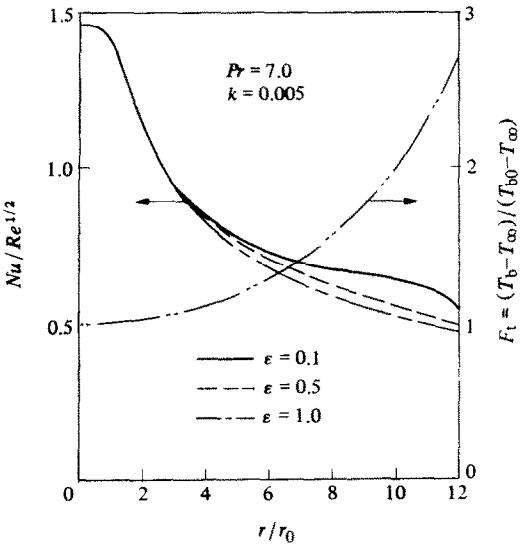

FIG. 6. Effect of the aspect ratio.

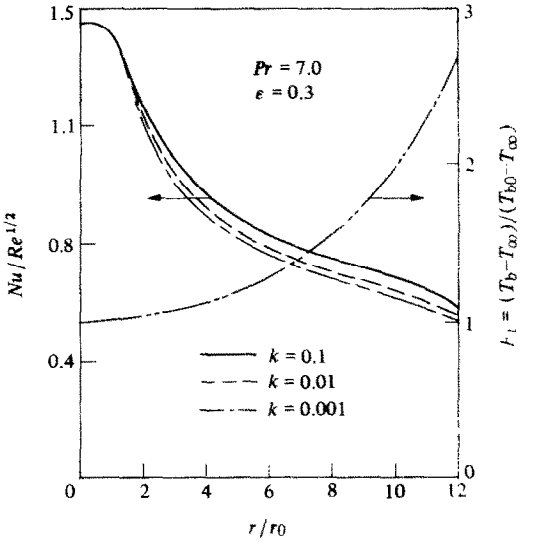

FIG. 7. Effect of the conductivity ratio.

according to the result of ref. [2]. On the other hand, when the prescribed temperature decreases with r, the interface temperature increases more slowly than that for a prescribed constant temperature. Consequently, the local Nusselt number becomes lower for the prescribed decreasing temperature. The prescribed heat flux distribution has a similar effect on the local Nusselt number.

The effect of the aspect ratio, ε, on the local Nusselt number profile is shown in Fig. 6 for a prescribed increasing temperature distribution. It is clear that the Nusselt number increases as ε is reduced towards the outer edge. This is because small values of ε correspond to thin disks and the effect of a prescribed temperature on the interface temperature is larger when the disk is thinner.

In order to examine the effect of the conductivity ratio, k, on the Nusselt number profile, the Nusselt number is calculated for different values of k and the results are shown in Fig. 7. It is evident that the local Nusselt number increases with the value of k. This is because a larger k represents a smaller solid conductivity. Hence the radial conduction in the solid phase is smaller so that the interface temperature increases with r more steeply. Consequently, the local Nusselt number becomes higher when k is larger.

5. CONCLUSIONS

The conjugate problem associated with laminar free jet impingement has been solved analytically. The heat transfer coefficient between the jet and the solid disk is influenced by the Prandtl number of the fluid, the ratio of the fluid conductivity to the solid conductivity and the ratio of the thickness to the radius of the disk as well as the prescribed temperature or heat flux profile. For the special case of vanishing ε, the present result is in good agreement with the previous result of ref. [2] in which the temperature or heat flux is prescribed at the interface. When the solid conductivity is sufficiently high, the prescribed heat flux has little influence on the Nusselt number distribution because of high radial conduction. It is found that for a very thick disk, the effect of the prescribed temperature or heat flux profile on the local heat transfer coefficient is negligible. For a thin disk, on the other hand, the prescribed temperature or heat flux profile has a considerable effect on the local heat transfer coefficient. Increasing the prescribed temperature or heat flux with r enhances the local Nusselt number while decreasing the prescribed temperature or heat flux with r reduces the local Nusselt number. The results also indicate that the local heat transfer coefficient becomes higher when k is larger.

REFERENCES

1. X. S. Wang, Z. Dagan and L. M. Jiji, Heat transfer between a circular free impinging jet and a solid surface with non-uniform wall temperature or wall heat flux—1. Solution for the stagnation region, *Int. J. Heat Mass Transfer* **32**, 1351–1360 (1989).
2. X. S. Wang, Z. Dagan and L. M. Jiji, Heat transfer between a circular free impinging jet and a solid surface with non-uniform wall temperature or wall heat flux—2. Solution for the boundary layer region, *Int. J. Heat Mass Transfer* **32**, 1361–1371 (1989).
3. Wen-Chien Lee and Yi-Hsu Ju, Conjugate Leveque solution for Newtonian fluid in a parallel plate channel, *Int. J. Heat Mass Transfer* **29**, 941–947 (1986).
4. A. V. Luikov, V. A. Aleksashenko and A. A. Aleksashenko, Analytical methods of solution of conjugated problems in convective heat transfer, *Int. J. Heat Mass Transfer* **14**, 1047–1056 (1971).
5. S. Ramadhyani, D. F. Moffat and F. P. Incropera, Conjugate heat transfer from small isothermal heat sources embedded in a large substrate, *Int. J. Heat Mass Transfer* **28**, 1945–1952 (1985).

6. A. V. Luikov, Conjugate convective heat transfer problems, *Int. J. Heat Mass Transfer* **17**, 257–265 (1974).
7. B. T. F. Chung and S. A. Kassemi, Conjugate heat transfer for laminar flow over a plate with a nonsteady temperature at the lower surface, *J. Heat Transfer* **102**, 177–180 (1980).
8. E. M. Sparrow and M. Faghri, Fluid-to-fluid conjugate heat transfer for a vertical pipe—internal forced convection and external natural convection, *J. Heat Transfer* **102**, 402–407 (1980).
9. V. E. Nakoryakov, B. G. Pokusaev and E. N. Troyan, Impingement of an axisymmetric liquid jet on a barrier, *Int. J. Heat Mass Transfer* **21**, 1175–1184 (1978).
10. E. M. Sparrow and C. Prakash, Interaction between internal natural convection in an enclosure and an external natural convection boundary-layer flow, *Int. J. Heat Mass Transfer* **24**, 895–907 (1981).
11. G. S. Barozzi and G. Pagliarini, A method to solve conjugate heat transfer problems: the case of fully developed laminar flow in a pipe, *J. Heat Transfer* **107**, 77–83 (1985).

TRANSFERT THERMIQUE CONJUGUE ENTRE UN JET LIQUIDE LAMINAIRE INCIDENT ET UN DISQUE SOLIDE

Résumé—On étudie analytiquement le transfert thermique conjugué entre un jet liquide laminaire incident et un disque isolé latéralement, avec une distribution arbitraire de température ou de flux donnée sur la face non frappée. Le nombre de Nusselt dépend localement du nombre de Prandtl *Pr* du fluide, du rapport des conductivités du fluide et du solide k, du rapport ε de l'épaisseur du disque au rayon, et de la distribution choisie. Pour un disque épais, par exemple $\varepsilon = 1$, la température (ou le flux choisi) a peu d'effet sur le coefficient local de transfert, mais l'effet est considérable pour un disque mince. Un accroissement suivant la distance radiale r du flux (ou de la température) augmente le coefficient local de transfert, alors qu'une décroissance provoque une diminution. Les résultats montrent aussi que le nombre de Nusselt local est plus important quand k est grand, les autres paramètres restant inchangés. Pour une très petite valeur de ε, soit $\varepsilon = 0{,}001$, le résultat est le même que si la condition à la limite était imposée sur la surface frappée (*Int. J. Heat Mass Transfer* **32**, 1361–1371 (1989)).

WÄRMEÜBERGANG ZWISCHEN EINEM LAMINAR AUFTREFFENDEN FLÜSSIGKEITSSTRAHL UND EINER SCHEIBE

Zusammenfassung—Der Wärmeübergang zwischen einem laminaren, frei auftreffenden Flüssigkeitsstrahl und einer seitlich isolierten Scheibe mit einer beliebig aufgeprägten Temperatur- oder Wärmestromdichten-Verteilung an der Rückseite wird analysiert. Die lokale Nusselt-Zahl zeigt sich dabei abhängig von der Prandtl-Zahl der Flüssigkeit, vom Verhältnis k zwischen den Wärmeleitfähigkeiten von Flüssigkeit und Scheibe, vom Verhältnis ε zwischen Dicke und Radius der Scheibe und der gewählten Temperatur- oder Wärmestromdichten-Verteilung. Für eine dicke Scheibe, z. B. $\varepsilon = 1$, hat die gewählte Temperatur- oder Wärmestromdichten-Verteilung nur einen geringen Einfluß auf den lokalen Wärmeübergangskoeffizienten. Für eine dünne Scheibe ist der Einfluß dagegen beträchtlich. Eine Erhöhung der Temperatur oder der Wärmestromdichte mit dem Abstand r vom Staupunkt erhöht den lokalen Wärmeübergangskoeffizenten. Die Ergebnisse zeigen außerdem, daß die Nusselt-Zahl mit steigendem k größer wird, wenn alle anderen Parameter konstant gehalten werden. Für sehr kleines ε, z. B. $\varepsilon = 0{,}001$, ist das Ergebnis im wesentlichen dasselbe wie in dem Fall, wenn die Randbedingung auf der Vorderseite aufgezwungen wird (*Int. J. Heat Mass Transfer* **32**, 1361–1371 (1989)).

СОПРЯЖЕННЫЙ ТЕПЛОПЕРЕНОС ПРИ НАТЕКАНИИ ЛАМИНАРНОЙ СТРУИ ЖИДКОСТИ НА ТВЕРДЫЙ ДИСК

Аннотация—Аналитически исследуется сопряженный теплоперенос между ламинарной свободно натекающей струей жидкости и диском с изолированной боковой поверхностью при произвольном распределении температуры или теплового потока на невзаимодействующей поверхности. Найдено, что локальное число Нуссельта зависит от числа Прандтля жидкости, *Pr*, отношения теплопроводностей жидкости и твердого диска, k, отношения толщины диска к его радиусу, ε, а также от заданного распределения температуры или теплового потока. В случае большой толщины диска, т.е. при $\varepsilon = 1$, заданные температура или тепловой поток оказывают незначительное влияние на локальный коэффициент теплопереноса. Для тонкого диска это влияние оказывается существенным. При росте заданной температуры или теплового потока с увеличением радиального расстояния r от точки торможения локальный коэффициент теплопереноса увеличивается, в то время как при снижении указанных величин с расстоянием r происходит его уменьшение. Результаты также показывают, что при увеличении значения k локальное число Нуссельта возрастает, а остальные параметры остаются неизменными. В случае очень малого значения ε, скажем, при $\varepsilon = 0.001$, результат принципиально не отличается от данных, полученных при наложении граничного условия на поверхность с натеканием струи.